

Electric Motor Design Optimization: A Convex Surrogate Modeling Approach [★]

Olaf Borsboom ^{*} Mauro Salazar ^{*} Theo Hofman ^{*}

^{*} Eindhoven University of Technology, 5600 MB, Eindhoven,
The Netherlands (e-mail: {o.j.t.borsboom, m.r.u.salazar,
t.hofman}@tue.nl).

Abstract: This paper instantiates a convex electric powertrain design optimization framework, bridging the gap between high-level powertrain sizing and low-level components design. We focus on the electric motor and transmission of electric vehicles, using a scalable convex motor model based on surrogate modeling techniques. Specifically, we first select relevant motor design variables and evaluate high-fidelity samples according to a predefined sampling plan. Second, using the sample data, we identify a convex model of the motor, which predicts its losses as a function of the operating point and the design parameters. We also identify models of the remaining components of the powertrain, namely a battery and a fixed-gear transmission. Third, we frame the minimum-energy consumption design problem over a drive cycle as a second-order conic program that can be efficiently solved with optimality guarantees. Finally, we showcase our framework in a case study for a compact family car and compute the optimal motor design and transmission ratio. We validate the accuracy of our models with a high-fidelity simulation tool and calculate the drift in battery energy consumption. We show that our model can capture the optimal operating line and the error in battery energy consumption is low. Overall, our framework can provide electric motor design experts with useful starting points for further design optimization.

Keywords: Electric vehicles, electric motors, optimal design, surrogate modeling, convex optimization

1. INTRODUCTION

Electric vehicles are increasingly pervading the market, providing users with a zero-emission solution to personal mobility (IEA, 2021). However, to accelerate the widespread adoption of these vehicles, there is room for improvement in their affordability and range (Paoli and Gül, 2022). Streamlining the design process of the electric (e-)powertrain is an important step towards this goal, which can be achieved by both reducing the time and cost of the technological development and converging towards better designs of the e-powertrain, accounting for the specific application. This is a difficult task, since the e-powertrain is a complex system that consists of strongly coupled components, namely the battery, the electric motor (EM), the transmission, and the final drive-differential unit, as shown in Fig. 1. Moreover, there is typically a large disparity between the high-level vehicle requirements that powertrain designers might impose (in terms of performance, cost and energy efficiency) and the low-level component design questions that are raised in this context. Specifically, optimizing the design of the EM has proven to be a challenge due to the high number of design variables and the multidisciplinary character of the problem (Bramerdorfer et al., 2018). To this day, in holistic powertrain design problems, the modeling is generally performed by using significant simplifications and assumptions to ensure the problem is computationally tractable. This is achieved, for instance, by linearly scaling the EM and its losses in the maximum torque and the mass, sacrificing accuracy (Silvas et al., 2016). However, implementing an optimization algorithm using accurate

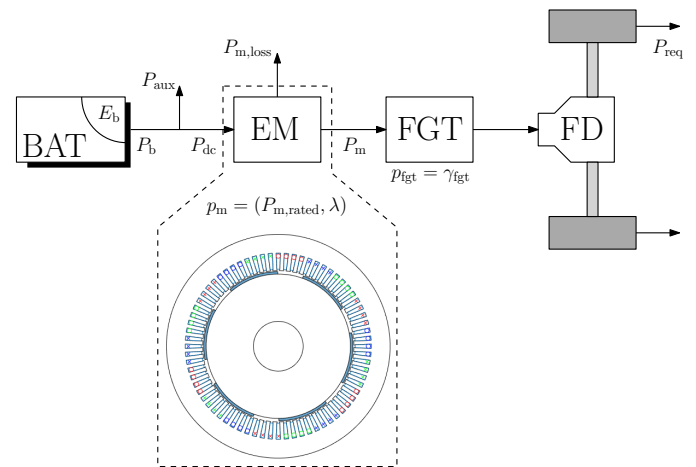


Fig. 1. A schematic layout of the electric powertrain. It consists of a battery pack (BAT), an electric motor (EM), a fixed-gear transmission (FGT) and a final drive-differential unit (FD) that is connected to the wheels. The arrows indicate the power flow between the components.

but computationally expensive models such as the finite element (FE) method, is not amenable to optimization.

This call for methods optimize the design of the e-powertrain with high accuracy, bridging the gap between high system-level sizing and low system-level design optimization of components. We need to account for a scaling of the components with more relevant parameters, accuracy and wider scaling ranges, whilst maintaining computational tractability.

[★] This publication is part of the project NEON (with project number 17628 of the research programme Crossover, which is (partly) financed by the Dutch Research Council (NWO)).

Against this backdrop, this paper presents a convex design optimization framework that leverages a scalable, convex EM optimization model based on surrogate modeling techniques.

Related literature: This work relates to three main research streams. The first stream considers the design optimization of EMs on a low system level. This issue is usually solved using FE-based approaches together with derivative-free optimization, but generally has a low-level objective, such as optimizing total harmonic distortion, torque ripple or power density (Lei et al., 2017; Bramerdorfer et al., 2018; Han et al., 2017). This does not connect well to the system-specific application (vehicle propulsion) and objective (powertrain energy consumption and cost).

The second stream considers the optimal sizing and control of (hybrid-)electric powertrains on a high system level. This problem is mainly addressed with derivative-free algorithms (Ebbesen et al., 2012; Hegazy and van Mierlo, 2010) or convex optimization (Murgovski et al., 2012; Borsboom et al., 2021; Silvas et al., 2016). However, as mentioned earlier, these methods require simplified scalable models for complex components that are usually only valid for limited scaling ranges ($\pm 10\text{-}20\%$ w.r.t. the maximum torque).

The final stream aims to connect the previous two research streams and comprises the design optimization of powertrains with more detailed EM models. The methods are based on either parametric regression models of high-fidelity data in a relatively large EM training set (Zhao, 2017), geometric scaling of a referent EM model (Ramakrishnan et al., 2018), or analytical design approaches (Krüger et al., 2022). However, all these methods lack global optimality guarantees and deal with high computational times. What is more, relatively large training sets require much effort from EM design engineers, whereas analytical models are specified for a particular EM (Hofman and Salazar, 2020).

In conclusion, to the best of the authors' knowledge, there are hardly any methods accounting for accurate EM design models in e-powertrain optimization in a computationally-efficient manner, giving accurate predictions over the whole design space, whilst limiting the efforts required by an EM design expert and still providing globally optimal solutions.

Statement of contributions: In order to address these challenges, this paper presents a convex optimization framework that optimizes the design of the EM and the transmission, based on surrogate modeling techniques. Specifically, we first derive a scalable, convex EM model that predicts the losses as a function of the geometric dimensions and the rated power, trained with data from a pre-defined sampling plan. Second, we leverage second-order conic programming to frame the minimum-energy consumption design problem, which minimizes the battery energy consumption of the e-powertrain over a drive cycle and computes the optimal EM design and transmission ratio. Third, to showcase our framework, we solve the problem on the WLTP cycle using nonlinear numerical solvers, providing a solution guaranteed to be globally optimal. Finally, we validate the accuracy of our solution with high-fidelity data.

Organization: This paper is organized as follows: Section 2 presents the EM surrogate model and the encompassing optimization problem, which contains models and constraint functions for the vehicle and the remaining powertrain components. We display our optimization frame-

work in Section 3, after which we draw the conclusions in Section 4, along with an outlook on future research.

2. METHODOLOGY

In this section, we construct the optimization problem by presenting convex constraints that describe the electric vehicle and its powertrain. We present the objective and the vehicle and component models in Sections 2.1–2.4 whereby we lay particular emphasis on the EM model, after which we summarize the problem in Section 2.5, followed by a discussion on the assumptions in Section 2.6.

The powertrain we consider in this paper, shown in Fig. 1, contains a battery, an EM, and a fixed-gear transmission (FGT) that is connected to the wheels via a final drive and a differential. In this work, we are jointly optimizing the design of the EM and the FGT.

2.1 Objective

The objective in our optimization problem is to minimize the internal energy consumption of the battery over a drive cycle:

$$\min \Delta E_b, \quad (1)$$

where ΔE_b is equal to the difference in battery state-of-energy (SOE), given by

$$\Delta E_b = E_b(0) - E_b(T), \quad (2)$$

where $E_b(0)$ and $E_b(T)$ are the SOE at the beginning and the end of the drive cycle, respectively.

2.2 Longitudinal Vehicle Dynamics and Transmission

In this section, we model the vehicle and the transmission. As is common practice in powertrain sizing studies, we adopt the quasi-static modeling approach (Guzzella and Sciarretta (2007)) in time domain. To keep our derivations succinct, we will drop the time dependence (t) whenever it is clear from the context. The power requested at the wheels P_{req} is equal to

$$P_{\text{req}} = v \cdot \left(\frac{1}{2} \cdot \rho_a \cdot c_d \cdot A_f \cdot v^2 + m_v \cdot (g \cdot c_r \cdot \cos(\alpha) + g \cdot \sin(\alpha) + a) \right),$$

where v , a and α are the velocity, acceleration and road inclination given by the drive cycle, respectively, ρ_a is the density of air, c_d is the drag coefficient, A_f is the frontal area, m_v is the mass of the vehicle, g is the Earth's gravitational constant, and c_r is the rolling resistance coefficient. We assume that the design of the EM does not significantly influence the total mass of the vehicle m_v , therefore we can compute P_{req} prior to the optimization.

We also assume that the FGT and the final drive have a constant efficiency. We only consider motor designs that can deliver the requested power, and we saturate the negative requested power with the maximum motor power $P_{\text{m,rated}}$. The mechanical motor power P_{m} , which we can also pre-compute, is then equal to

$$P_{\text{m}} = \begin{cases} \frac{1}{\eta_{\text{fgt}} \cdot \eta_{\text{fd}}} \cdot P_{\text{req}} & \text{if } P_{\text{req}} \geq 0 \\ \max(-P_{\text{m,rated}}, \eta_{\text{fgt}} \cdot \eta_{\text{fd}} \cdot r_b \cdot P_{\text{req}}) & \text{if } P_{\text{req}} < 0, \end{cases}$$

where η_{fgt} and η_{fd} are the efficiencies of the FGT and final drive, respectively, and r_b is the regenerative braking fraction.

We optimize the FGT ratio γ_{fgt} , which is bounded by

$$\gamma_{\text{fgt}} \in [\gamma_{\text{fgt}}^{\min}, \gamma_{\text{fgt}}^{\max}], \quad (3)$$

where $(\cdot)^{\min}$ and $(\cdot)^{\max}$ are the minimum and maximum values of the design variables. The input speed of the transmission, which is identical to the output speed of the EM ω_m , is equal to

$$\omega_m = \gamma_{\text{fgt}} \cdot \gamma_{\text{fd}} \cdot \frac{v}{r_w}, \quad (4)$$

where γ_{fd} is the ratio of the final drive and r_w is the radius of the wheels. We ensure the vehicle can reach the maximum velocity v_{max} by

$$\gamma_{\text{fgt}} \leq \omega_{m,\text{max}} \cdot \frac{r_w}{v_{\text{max}}}, \quad (5)$$

where $\omega_{m,\text{max}}$ is the maximum speed of the motor. We also require the vehicle to be able to launch from standstill on a road inclination angle α by the following constraint:

$$\gamma_{\text{fgt}} \geq m_v \cdot g \cdot r_w \cdot \sin(\alpha_{\text{max}}) \cdot \frac{1}{\eta_{\text{fgt}} \cdot \eta_{\text{fd}} \cdot T_{m,\text{max}}}, \quad (6)$$

where $T_{m,\text{max}}$ is the maximum torque of the motor.

2.3 Electric Motor

In this section, we derive a model of the EM. As mentioned in Section 1, this work focuses on creating an accurate scalable model of the EM, whereby we draw inspiration from classical surrogate modeling techniques, whilst preserving convexity. The goal of the EM model is to predict the motor losses $P_{m,\text{loss}}$ as a function of the operating point and the design variables

$$P_{m,\text{loss}} = f(P_m, \omega_m, p_m),$$

where p_m is the set of EM design variables.

To construct the surrogate model, we require high-fidelity samples of EMs. To this end, we use the open-source analytical tool MEAPA by Kalt et al. (2020), which is developed for the design and analysis of permanent magnet synchronous and asynchronous induction motors. In this work, we focus on surface-mounted permanent magnet motors, with a fixed rated voltage U , rated speed $\omega_{m,\text{rated}}$ and number of pole pairs n_p . The design variables we consider are the rated power $P_{m,\text{rated}}$ and the relative length λ . The relative length can be interpreted as the ratio between the length and the radius of the motor (measured at the stator's inner circumference between two poles), specifically given by

$$\lambda = \frac{l_s \cdot 2 \cdot n_p}{\pi \cdot D_{s,i}},$$

where l_s is the length and $D_{s,i}$ is the inner diameter of the stator.

Sampling Plan and Surrogate Model Formulation To construct our scalable surrogate model, we perform high-fidelity evaluations on specific locations in the design space, according to a predefined sampling plan. The design space is bounded by

$$\lambda \in [\lambda^{\min}, \lambda^{\max}] \quad (7)$$

$$P_{m,\text{rated}} \in [P_{m,\text{rated}}^{\min}, P_{m,\text{rated}}^{\max}]. \quad (8)$$

The specific sampling plan we select in this work, is a 3-level 2-factor Full Factorial sampling plan. The locations of the samples in the design space are shown in Fig. 2.

Using the high-fidelity data we acquired after evaluating the EMs in the sampling plan, we construct a convex, scalable surrogate model of the EM. The EM model formulation is inspired by previous work, see Borsboom

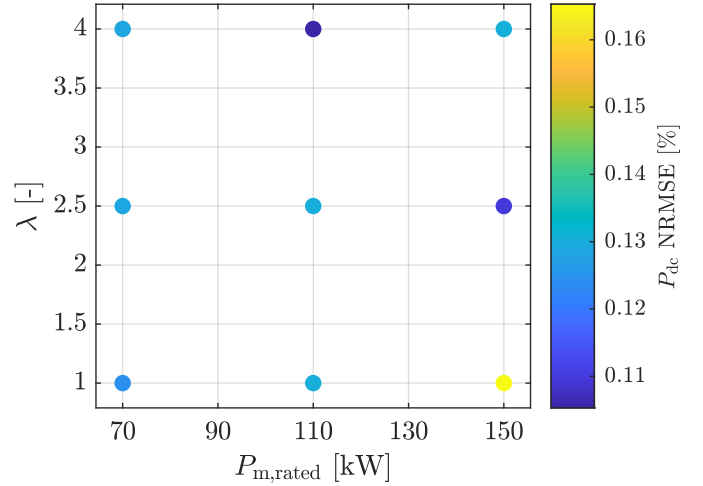


Fig. 2. The EM sampling locations within the design space, evaluated with the MEAPA tool, following a 3-level 2-factor Full Factorial sampling plan. The NRMSE of P_{dc} for each sample is visible in the color bar, with the mean NRMSE for all samples equal to 0.13%.

et al. (2021), with the addition of design variables. The electrical power P_{dc} is equal to

$$P_{\text{dc}} = P_m + P_{m,\text{loss}}. \quad (9)$$

As mentioned before, we can pre-compute the required mechanical power exerted by the EM P_m , hence we treat it as a given, exogenous parameter. We train the model of the losses for N different levels of $P_m \in [0, P_{m,\text{rated}}^{\min}]$, see van den Hurk and Salazar (2021); Korzilius et al. (2021). We express the motor losses, after relaxing the constraint, as

$$P_{m,\text{loss},i} \geq x_m^\top Q_{m,i} x_m \quad \forall i \in [1, \dots, N], \quad (10)$$

where $Q_{m,i}$ is a matrix of fitting coefficients subject to identification, determined for each level of P_m . For power levels in between the fitted values, we linearly interpolate the fitting coefficients. Vector x_m , which contains constant values, main factors, first-order interactions, and quadratic terms, is equal to

$$x_m = [1, \omega_m, P_{m,\text{rated}}, \lambda, \omega_m \cdot P_{m,\text{rated}}, \omega_m \cdot \lambda, P_{m,\text{rated}} \cdot \lambda, \omega_m^2, P_{m,\text{rated}}^2, \lambda^2].$$

To preserve convexity, we have relaxed the constraint in (10) and ensure that Q_i are positive semi-definite matrices, see Parrilo (2004). Given the objective in (1), the constraint in (10) will always hold with equality. After we determine values for the coefficients using semi-definite programming as in Borsboom et al. (2021), we can assess the quality of the model by inserting the same design parameters as in the sampling plan for the operational envelope, up to P_m^{\min} . The normalized root-mean-squared error (NRMSE) of predicting P_{dc} is visible for each sample in Fig. 2, resulting in a mean NRMSE for all samples equal to 0.13%. The efficiency maps of the data points and the predictions are shown in Fig. 3.

We ensure the motor is powerful enough to complete the drive cycle with the following constraint:

$$-P_{m,\text{rated}} \leq P_m \leq P_{m,\text{rated}}, \quad (11)$$

We determine the maximum torque $T_{m,\text{max}}$ from

$$T_{m,\text{max}} \leq \frac{P_{m,\text{rated}}}{\omega_{m,\text{rated}}}, \quad (12)$$

which we implement into our framework, in both motoring and regenerating mode, by

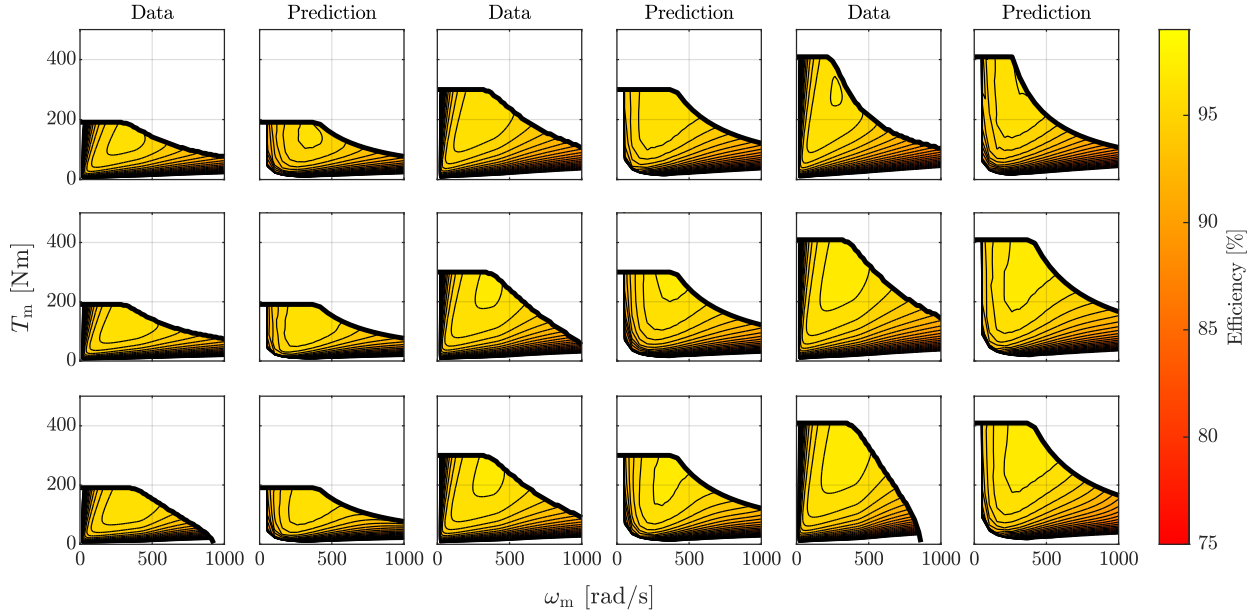


Fig. 3. The efficiency maps of all sampled data points, along with the efficiencies predicted by the EM model.

$$T_{m,\max} \cdot \gamma_{\text{fgt}} \cdot \eta_{\text{fgt}} \cdot \eta_{\text{fd}} \geq \frac{P_{\text{req}} \cdot r_w}{v} \quad (13)$$

$$T_{m,\max} \cdot \gamma_{\text{fgt}} \cdot \frac{1}{\eta_{\text{fgt}} \cdot \eta_{\text{fd}}} \geq \frac{P_{\text{req}} \cdot r_w}{v}. \quad (14)$$

In constraint (12), $T_{m,\max}$ can relax, but we allow it since it sets an upper bound for the torque of the motor.

2.4 Battery

In this section, we derive a model of the battery pack. The output power of the battery P_b is equal to

$$P_b = P_{\text{dc}} + P_{\text{aux}}, \quad (15)$$

where P_{aux} is the auxiliary power. Using the battery data from the quasi-static modeling toolbox in (Guzzella and Sciarretta, 2007), we model the internal battery power, after relaxation, as

$$P_1 \geq b_0 + b_1 \cdot P_b + b_2 \cdot P_b^2, \quad (16)$$

where b_0 , b_1 and b_2 are parameters subject to identification, with a resulting NRMSE of 1.23%. The battery SOE changes with P_1 as

$$\frac{d}{dt} E_b = -P_1. \quad (17)$$

We bound the battery SOE with the state-of-charge limits as

$$E_b \in [\zeta_b^{\min}, \zeta_b^{\max}] \cdot E_{b,\max}, \quad (18)$$

where $E_{b,\max}$ is the predetermined total battery capacity—and thus not an optimization variable—and ζ_b^{\min} and ζ_b^{\max} are the minimum and maximum state-of-charge levels, respectively. We assume that the vehicle starts the drive cycle with a fully charged battery

$$E_b(0) = \zeta_b^{\max} \cdot E_{b,\max}. \quad (19)$$

2.5 Optimization Problem

In this section, we summarize the optimal design problem. The state variable is $x = E_b$. The design variables are $p = (P_{m,\text{rated}}, \lambda, \gamma_{\text{fgt}})$.

Problem 1. (Nonlinear Convex Problem). The minimum-energy design is the solution of

$$\begin{aligned} \min \quad & \Delta E_b \\ \text{s.t.} \quad & (2) - (19). \end{aligned}$$

Although Problem 1 is convex, it cannot be solved with standard convex solvers. However, we can compute the solution, which is still guaranteed to be globally optimal, using nonlinear solvers.

2.6 Discussion

A few comments are in order. First, we assume that the mass of the EM does not significantly impact the total mass of the vehicle, enabling us to pre-compute P_{req} . In fact, the mass of the motor will change with $P_{m,\text{rated}}$, yet its contribution to the total mass of the vehicle is relatively small and can be neglected (Grunditz and Thiringer, 2018). Second, in the training data set, some motors with a small value for λ have to reduce the power at high rotational speeds in order to not exceed the limits of the circumferential rotor speed and the flux linkage. However, since vehicles in this application hardly operate in this region of the envelope, it is considered of minor influence when optimizing the motor size in this stage of development. Third, we assume a constant efficiency of the FGT, which is in line with common practice (Verbruggen et al., 2020), and we assume that the cooling system can cope with the heating of the motor (Konda et al., 2022). Fourth, we have focused on two design variables for the EM, whilst the low-level design space for motors can be of a higher dimension. Yet, our framework can be readily extended to account for more design parameters. In the case that more design parameters are selected, the Full Factorial sampling plan—given its exponential characteristic in the number of parameters—can be replaced by Latin Hypercube, Central Composite or Box-Behnken sampling plans (Garud et al., 2017).

3. RESULTS

In this section, we present the numerical results obtained when we apply the optimization models presented in

Table 1. Vehicle Parameters

Parameter	Symbol	Value	Units
Wheel Radius	r_w	0.35	[m]
Air drag coefficient	c_d	0.29	[-]
Frontal Area	A_f	2.38	[m ²]
Air density	ρ_a	1.2041	[kg/m ³]
Rolling resistance coefficient	c_{rr}	0.0174	[-]
Gravitational constant	g	9.81	[m/s ²]
Brake fraction	r_b	0.6	[-]
Final drive ratio	γ_{fd}	1	[-]
Vehicle mass	m_v	1,850	[kg]
Auxiliary power	P_{aux}	2	[kW]
Maximum SoC	ζ_b^{\max}	0.80	[-]
Minimum SoC	ζ_b^{\min}	0.20	[-]

Table 2. Powertrain Parameters

Parameter	Symbol	Value	Units
<i>Electric Motor</i>			
Voltage	U	700	[V]
Rated speed	$\omega_{m,rated}$	3,500	[rpm]
Maximum speed	$\omega_{m,max}$	10,000	[rpm]
Number of pole pairs	n_p	3	[-]
Relative length bounds	λ^{\max}	4	[-]
	λ^{\min}	1	[-]
Rated power bounds	$P_{m,rated}^{\max}$	150	[kW]
	$P_{m,rated}^{\min}$	70	[kW]
<i>Fixed-gear Transmission</i>			
Motor to Wheel Efficiency	$\eta_{fgt} \cdot \eta_{fd}$	0.96	[-]
FGT ratio limits	γ_{fgt}^{\max}	10	[-]
	γ_{fgt}^{\min}	1	[-]
Maximum velocity	v_{max}	160	[km/h]
Maximum launch inclination	α_{max}	20	[°]

Section 2 to the EM design of a compact car. We optimize the design of the EM for the Worldwide Harmonized Light Vehicle Test Cycle (WLTC) Class 3. Table 1 shows the vehicle parameters for which the optimal design is obtained. The EM and FGT specifications are summarized in Table 2. Since our system dynamics (E_b) are captured by an open integrator, we discretize the optimization problem with a sampling time of 1s using the forward Euler method. In the case of closed-loop state dynamics (for instance in thermal modeling), other discretization methods could be necessary (Locatello et al., 2021). We parse the problem with CasADi (Andersson et al., 2019) and solve it with the nonlinear solver IPOPT (Wachter and Biegler, 2006). Because the problem is still convex, we preserve global optimality guarantees, since any KKT point found is a global minimum (Boyd and Vandenberghe, 2004). Parsing the optimal design problem and solving it both take around 7s. All computations are performed on an Intel Core i7-1065G7 CPU and 16.0 GB of RAM.

3.1 Numerical Results

After solving the optimal design problem for the parameters in Tables 1 and 2, we arrive at an optimal design solution of $P_{m,rated} = 145$ kW, $\lambda = 3.49$, $\gamma_{fgt} = 5.7$. This is in line with current power ratings of electric vehicles with similar specification, such as the Volkswagen ID.3, which is rated at 150 kW (Volkswagen, 2019). The efficiency map and limits predicted by the EM model of the solution design are shown in Fig. 4. The predicted trajectories in terms of $P_{m,loss}$ and the battery SOE E_b are shown in Fig. 5.

3.2 Validation

In order to validate our models, we feed the obtained design values in the MEAPA tool and carry out the

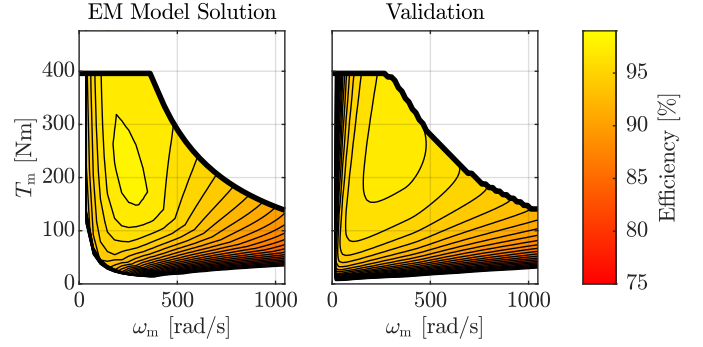


Fig. 4. The efficiency map predicted by the EM model in the optimal solution ($P_{m,rated} = 145$ kW, $\lambda = 3.49$) is shown in the left subplot. On the right, the EM generated by the MEAPA tool for the same design as in the solution, serving as a design validation.

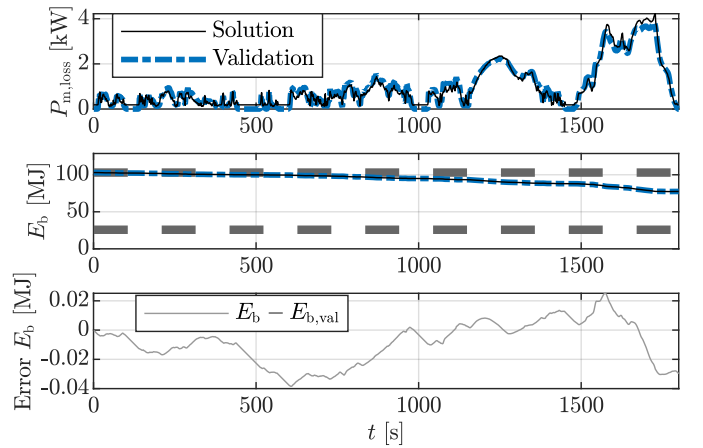


Fig. 5. The trajectories of $P_{m,loss}$ and E_b , from both the optimal solution and validation. In the bottom subplot, the battery energy error in E_b is indicated.

analysis. The resulting efficiency map is shown in the right subplot of Fig. 4. Although the EM model prediction can more accurately capture the full efficiency map in the sampling points (Fig. 3), the EM prediction of the solution in the left subplot of Fig. 4 can seize the optimal operating line relatively well. To further quantify the modeling accuracy, we feed the obtained trajectories on the drive cycle from the solution through the nonlinear efficiency maps of the validation. The resulting $P_{m,loss}$ and the impact of it on E_b are shown in Fig. 5. The bottom subplot shows the error in battery energy consumption E_b , which is quantified as the difference between the SOE trajectory from the solution (E_b) and the validation ($E_{b,val}$). At the end of the drive cycle, the error is equal to 30 kJ, which corresponds to 0.12% w.r.t. the energy consumed. This shows that the framework is capable of accurately predicting the losses of an optimally sized scalable motor.

4. CONCLUSIONS

In this paper, we proposed to bridge the gap between high-level powertrain sizing and low-level EM design, and instantiated a convex optimization framework for the design of an electric motor (EM) and a fixed-gear transmission, which incorporates accurate scaling of the EM. To this end, we took inspiration from surrogate modeling techniques and applied the ideas to predicting the losses of an EM as a function of its design, whilst preserving convexity. After computing the energy-optimal design given a drive cycle, we compared the solution with

the data obtained from the high-fidelity tool for the same design. We observed that the predicted efficiency maps behave only slightly differently, the optimal operating line was captured well, with a relatively small error in energy consumption over a drive cycle of 0.21%. Therefore, this optimization model can aid EM design experts by providing them with a promising starting point, from which they can further refine the low-level design of EMs for automotive applications.

This work opens the field to future research lines: First of all, the accuracy of the model over the full design space—specifically, at the candidate optimum—could be improved by adding an iterative nature to the optimization procedure. Namely, the use of infill points based on particular criteria can further explore the design space or refine the model in the solution (Forrester et al., 2008). Second, the model can be extended by including additional design variables.

ACKNOWLEDGEMENTS

We thank Dr. Ilse New for proofreading this paper.

REFERENCES

- Andersson, J.A.E., Gillis, J., Horn, G., Rawlings, J.B., and Diehl, M. (2019). Casadi – a software framework for non-linear optimization and optimal control. *Mathematical Programming Computation*, 11(1), 1–36.
- Borsboom, O., Fahdzyana, C.A., Hofman, T., and Salazar, M. (2021). A convex optimization framework for minimum lap time design and control of electric race cars. *IEEE Transactions on Vehicular Technology*, 70(9), 8478–8489.
- Boyd, S. and Vandenberghe, L. (2004). *Convex optimization*. Cambridge Univ. Press.
- Bramerdorfer, G., Tapia, J., Pyrhönen, J.J., and Cavignino, A. (2018). Modern electrical machine design optimization: Techniques, trends, and best practices. *IEEE Transactions on Industrial Electronics*, 65(10), 7672–7684.
- Ebbesen, S., Dönitz, C., and Guzzella, L. (2012). Particle swarm optimization for hybrid electric drive-train sizing. *International Journal of Vehicle Design*, 58(2–4), 181–199.
- Forrester, A.I.J. and Keane, A.J. (2009). Recent advances in surrogate-based optimization. *Progress in Aerospace Sciences*, 45, 50–79.
- Forrester, A.I.J., Sóbester, A., and Keane, A.J. (2008). *Engineering Design via Surrogate Modeling: A Practical Guide*. John Wiley & Sons, first edition.
- Garud, S.S., Karimi, I.A., and Kraft, M. (2017). Design of computer experiments: A review. *Computers and Chemical Engineering*, 106, 71–95.
- Grunditz, E.A. and Thiringer, T. (2018). Electric vehicle acceleration performance and motor drive cycle energy efficiency trade-off. In *IEEE Int. Conf. on Electric Machines*.
- Guzzella, L. and Sciarretta, A. (2007). *Vehicle propulsion systems: Introduction to Modeling and Optimization*. Springer Berlin Heidelberg, second edition.
- Han, W., Dang, C., Kim, J.W., Kim, Y.J., and Jung, S.Y. (2017). Global-simplex optimization algorithm applied to FEM-based optimal design of electric machine. *IEEE Transactions on Magnetics*, 53(6).
- Hegazy, O. and van Mierlo, J. (2010). Particle swarm optimization for optimal powertrain component sizing and design of fuel cell hybrid electric vehicle. In *Int. Conf. on Optimization of Electrical and Electronic Equipment*.
- Hofman, T. and Salazar, M. (2020). Transmission ratio design for electric vehicles via analytical modeling and optimization. In *IEEE Vehicle Power and Propulsion Conference*.
- IEA (2021). Global EV outlook 2021. Technical report, International Energy Agency.
- Kalt, S., Ehrhard, J., and Lienkamp, M. (2020). Electric machine design tool for permanent magnet synchronous machines and induction machines. *Machines*, 8(15).
- Konda, M., Hofman, T., and Salazar, M. (2022). Energy-optimal design and control of electric powertrains under motor thermal constraints. In *European Control Conference*. In press. Available online at <https://arxiv.org/abs/2111.07711>.
- Korzilius, O., Borsboom, O., Hofman, T., and Salazar, M. (2021). Optimal design of electric micromobility vehicles. In *Proc. IEEE Int. Conf. on Intelligent Transportation Systems*. In press. Extended version available at <https://arxiv.org/abs/2104.10155>.
- Krüger, B., Keinprecht, G., Filomeno, G., Dennin, D., and Tenberge, P. (2022). Design and optimisation of single motor electric powertrains considering different transmission topologies. *Mechanism and Machine Theory*, 168.
- Lei, G., Zhu, J., Gou, Y., Liu, C., and Ma, B. (2017). A review of design optimization methods for electrical machines. *Energies*, 10(12).
- Locatello, A., Konda, M., Borsboom, O., Hofman, T., and Salazar, M. (2021). Time-optimal control of electric race cars under thermal constraints. In *European Control Conference*.
- Murgovski, N., Johannesson, L., Sjöberg, J., and Egardt, B. (2012). Component sizing of a plug-in hybrid electric powertrain via convex optimization. *Mechatronics*, 22(1), 106–120.
- Paoli, L. and Gül, T. (2022). Electric cars fend off supply challenges to more than double global sales. Available at <https://www.iea.org/commentaries/electric-cars-fend-off-supply-challenges-to-more-than-double-global-sales>.
- Parrilo, P.A. (2004). Sum of squares programs and polynomial inequalities. *SIAG/OPT Views-and-News*, 15(2), 7–15.
- Ramakrishnan, K., Stipetic, S., Gobbi, M., and Mastinu, G. (2018). Optimal sizing of traction motors using scalable electric machine model. *IEEE Transactions on Transportation Electrification*, 4(1), 314–321.
- Silvas, E., Hofman, T., Murgovski, N., Etman, P., and Steinbuch, M. (2016). Review of optimization strategies for system-level design in hybrid electric vehicles. *IEEE Transactions on Vehicular Technology*, 66(1), 57–70.
- van den Hurk, J. and Salazar, M. (2021). Energy-optimal design and control of electric vehicles’ transmissions. In *IEEE Vehicle Power and Propulsion Conference*. In press. Extended version available at <https://arxiv.org/abs/2105.05119>.
- Verbruggen, F.J.R., Salazar, M., Pavone, M., and Hofman, T. (2020). Joint design and control of electric vehicle propulsion systems. In *European Control Conference*.
- Volkswagen (2019). Vision made reality: wold premiere of the ID.3. Available at <https://www.volkswagen-newsroom.com/en/press-releases/vision-made-reality-world-premiere-of-the-id3-5338>.
- Wachter, A. and Biegler, L.T. (2006). On the implementation of an interior-point filter line-search algorithm for large-scale nonlinear programming. *Mathematical Programming*, 106(1), 25–57.
- Zhao, J. (2017). *Design and Control Co-Optimization for Advanced Vehicle Propulsion Systems*. Ph.D. thesis, Université Paris-Scalay, IFP Energies Nouvelles.